



Numerical analysis of energy dissipator options using computational fluid dynamics modeling — a case study of Mirani Dam

Usama Majeed¹ · Najam us Saqib² · Muhammad Akbar³

Received: 16 June 2022 / Accepted: 2 October 2022 / Published online: 15 October 2022
© Saudi Society for Geosciences 2022

Abstract

In this study, the FLOW 3D computational fluid dynamics (CFD) software was used to estimate the performance of the United States Bureau of Reclamation (USBR) type II and USBR type III stilling basins as energy dissipation options for the Mirani Dam spillway, Pakistan. The 3D Reynolds-averaged Navier–Stokes equations were solved, which included sub-grid models for air entrainment, density evaluation, and drift–flux, to capture free-surface flow over the spillway. Five models were considered in this research. The first model has a USBR type II stilling basin with a length of 39.5 m. The second model has a USBR type II stilling basin with a length of 44.2 m. The 3rd and 4th models have a USBR type II stilling basin with a length of 48.8 m and a 39.5 m USBR type III stilling basin, respectively. The fifth model is identical to the fourth, but the friction and chute block heights have been increased by 0.3 m. To set up the best FLOW 3D model conditions, mesh sensitivity analysis was performed, which yielded a minimum error at a mesh size of 0.9 m. Three sets of boundary conditions were tested and the set that gave the minimum error was employed. Numerical validation was done by comparing the physical model energy dissipation of USBR type II ($L = 48.8$ m), USBR type III ($L = 35.5$ m), and USBR type III with 0.3-m increments in blocks ($L = 35.5$ m). The statistical analysis gave an average error of 2.5% and a RMSE (root mean square error) index of less than 3%. Based on hydraulics and economic analysis, the 4th model was found to be an optimized energy dissipator. The maximum difference between the physical and numerical models in terms of percentage energy absorbed was found to be less than 5%.

Keywords Numerical modeling · Spillway · Hydraulic jump · Energy dissipation · FLOW 3D

Introduction

A crucial appurtenant to every dam or reservoir is a spillway and stilling basins that serve to safely discharge any additional excess water from the structure which the dam's reservoir is unable to hold (Saqib et al. 2022a). Spillways and stilling basins are important to the dam because they can cause the dam to be overtopped, resulting in partial or complete dam failure (Raza et al. 2021). Overflowing water from a dam spillway can damage the structure, putting it at risk of failure or producing catastrophic conditions (Saqib et al. 2021). The water speeds up as it descends over the spillway's crest (Reeve et al. 2019). There may be dangerous scour in the natural channel below this construction because of the high velocity of the spillway face at the spillway toe (Li et al. 2019). The spillway's primary function is to reduce the water's kinetic energy, and the stilling basin contains the water if there is any kinetic energy left. To reduce kinetic energy or head loss, a variety of spillways have been developed over the years.

Responsible Editor: Broder J. Merkel

✉ Muhammad Akbar
akbarmohammad0092@gmail.com

Usama Majeed
Engr.usama@uet.edu.pk

Najam us Saqib
najam.fraz@gmail.com

¹ University of Engineering and Technology, Lahore 54700, Pakistan

² Faculty of Engineering, Lahore Leads University, Lahore 54700, Pakistan

³ Institute of Mountain Hazards and Environment, Chinese Academy of Sciences, Chengdu 61004, China

Common types of spillways include ogee spillways, stepped spillways, morning glory spillways, and labyrinth spillways (Rong et al. 2019). This change in spillway geometry was made to reduce the length of the stilling basin. However, due to a variety of constraints, stilling basins are added downstream of the spillways. Previously, physical modeling was used to obtain information about the hydraulics of flow for hydraulic structures, which included rating curves, pressure over the spillway, water elevation, velocity along the length of the hydraulic structure, and requirement of stilling basins. Sorensen (1986) made studies on spillway models comparing ogee and stepped spillways and found that stepped spillways provide more resistance to flow. Rice and Kadavy (1996) did studies on lower scale models and found that energy dissipation is more in stepped spillways, as compared to ogee smooth spillways. Nangare and Kote (2017) attempted to build an ogee profile stepped spillway for the Khadakwasla dam with a plain and slotted roller bucket as an energy dissipator. The laboratory tests included four combinations of ogee profile stepped spillways with plain and slotted roller buckets. At 6 m head, the stepped spillway with a slotted roller bucket model (SSRB) dissipated the most specific energy (83.36%). Asaram et al. (2016) evaluated the impact of the varied slopes of the ogee spillway surface on energy dissipation. Three ogee spillway models were created with slopes of 1:1, 0.85:1, and 0.75:1. Eighteen test runs were done to figure out how much energy was lost after the three spillway models.

Computational fluid dynamics (CFD) solves fluid flow problems using empirical equations (Versteeg and Malalasekera 1979). In recent years, CFD has been utilized to estimate flow conditions for hydraulic structures. CFD makes it easy to generate rating curves and detailed velocity profiles for complex hydraulic structures. Amorim et al. (2015) developed a physical model of the Porto Colombia Hydropower Plant to study hydraulic jumps in the stilling basin. Pressure and water surface levels were computed over the spillway and stilling basin at a 4000-m³/s discharge in the physical model. A numerical model was validated by comparing results with the prototype and physical model data. Computed pressure and water surface levels at 4000 m³/s discharge by numerical models were compared with a physical model that showed good agreement of results with each other. Kumcu (2017) performed physical modeling of two ogee spillways having scale 1:30 and 1:3 of prototype, respectively. The water level and the pressure were measured by the physical model placed in a laboratory flume. The results of 3D numerical model results as compared to the 2D model showed less difference with physical model data. Valero et al. (2016) investigated USBR basin type III, considering a smooth chute and a stepped chute in the spillway. The numerical model for both scenarios was simulated using FLOW 3D. In the smooth chute, turbulence

was developed by chute blocks, which increased the turbulence of the hydraulic jump impact point. On the other hand, the stepped chute continuously created turbulence along the spillway which decreased the turbulence of the hydraulic jump impact point. Moreover, the structure was analyzed for the worst tailwater conditions to dissipate the energy of the water to avoid damage to the downstream bed. Serafeim et al. (2015) investigated flow conditions over an ogee weir using physical modeling and compared them with a numerical model using CFD software. A comparison of water surface levels obtained using physical modeling and a CFD model was made, which showed good agreement with each other.

Ho and Riddette (2010) used computational fluid dynamics to upgrade several spillways in Australia to efficiently pass increased floods to avoid damages downstream of the river. Models were validated by comparing the computed result with published data for the precision of output data. The researcher encourages the utilization of CFD techniques due to time-saving and cost-effectiveness. Damiron (2015) numerically simulated the Bergeforsen dam with aerators and without aerators at different discharges. Model results revealed that the risk of cavitation before the stilling basin was at its minimum, and 20 m away from the threshold was at its maximum. Despite that, water surface levels, velocity profiles, and pressure were also computed using the numerical model. A comparison of the numerical model and the physical model was made to access the capability of the software. Dunlop et al. (2016) modified the spillway of the Cabinet Gorge Dam to minimize total dissolved gas, which affects the quality of water. The single bay of spillways was modeled using the computational fluid dynamics software Flow 3D. The roughness elements were introduced to optimize the bay of the spillway to minimize total dissolved gas at the spillway's downstream side. Different scenarios and layouts were modeled in FLOW 3D considering the decrease in total dissolved gas, spillway capacity, and construction simplicity. Herrera-Granados and Kostecki (2016) carried out a study due to the changes in the flow condition of the Niedow barrage located in southern Poland. The 2D numerical model was developed to obtain water surface level and average velocities in the reservoir, which were further utilized as boundary conditions of the 3D model. The discharge coefficient was measured with and without a coffer dam using a numerical model and a laboratory physical model and then these obtained discharge coefficients were compared with the value proposed by USBR. The discharge coefficient values for low flows were overestimated as compared to those proposed by USBR. Fleit et al. (2018) used CFD to simulate flow conditions over an ogee-crested weir. The numerical model was validated using laboratory experiments. The model was simulated for a free-floating and submerged scenario. The upstream head above the

ogee crest weir was computed at different flow rates using the physical model and a numerical model with the free-floating condition. The difference between the upstream head predicted by the physical and numerical models was less than 3%. Muthukumaran and Prince Arulraj (2020) reviewed the impact of using nanomaterials to increase the energy dissipation and discharge capacity of the spillway. For this purpose, they did physical modeling and used the rectangular flume for the research investigation. Kocaer and Yazar (2020) used ANSYS-Fluent and OpenFOAM to simulate the flow depths over the ogee spillways. They experimented with the flows in the rectangular flume and compared the readings with the numerical model. It was found that they matched well. Pasbani Khiavi et al. (2021) altered the geometry of ogee spillways and checked its capability by introducing the steps using ANSYS CFX software. In this study, the finite volume method based on elements was applied for modeling and the SIMPLE iterative algorithm was applied to couple the velocity and pressure terms. It was found that simple ogee spillways dissipated only 55%, as compared to 80% in stepped spillways. Saqib et al. (2022a) used the latest CFD software, FLOW 3D, to look for energy dissipation across the simple stepped spillway models. For validation, authors adopted results from a previously published paper and found that these agreed well with the FLOW 3D. Spillways and stilling basins are crucial because they affect the safety of the dams, as previously discussed. Furthermore, damage to property and loss of life may result from the spillways and stilling basins failing. The effectiveness of spillways and stilling basins at the maximum flow rates therefore must be investigated, as well as the amount of energy lost. The goal of the current study is to assess different energy dissipation options for the Mirani Dam in terms of available stilling basin options. The study is further aimed at proposing the most effective stilling basins in terms of hydraulics and cost analysis.

Materials and methods

Mirani Dam

Mirani Dam was selected for this particular study. It is the first rock-fill dam in Pakistan. The reasons behind this are (1) availability of data, and (2) dam and spillway size that were equivalent to the CFD capacity available. At a distance of roughly 30 mi (48 km) west of Turbat and 380 mi (610 km) southwest of Quetta, the Mirani Dam is located on the Dasht River in the Makran Division of the Baluchistan province of Pakistan. The Central Makran Range may be found to the north of the dam site, on the other side of the river. The dam is located in Kaur-e-Awaran, approximately 7 km (4.3 mi) downstream of the confluence of the two major

tributaries of the Dasht River, the Kech River, and the Nihing River. As seasonal streams, the Kech and the Nihing receive their water from rainfall and snowmelt from the mountains upstream during the summer months. Figure 1 presents the layout and location of Mirani Dam. Some of the important parameters of Mirani Dam are presented in Table 1. The engineering drawing of the plan and cross section were adopted by WAPDA (Water and Power Development Authority). They are presented in Figs. 2, 3, 4, and 5.

Numerical methodology

FLOW Science has developed three-dimensional software FLOW 3D for simulating fluid flow problems (Parsaie et al. 2018). FLOW 3D utilizes the volume of fluid technique with a well-defined grid. This has been widely used for the analysis of hydraulic structures due to its easy graphic user interface (GUI) and good agreement of results with the physical model and prototype.

FLOW 3D uses the Reynolds-averaged Navier–Stokes equation and calculates the portion of the fluid in each cell to predict the movement of fluid over the free surface (Naderi et al. 2019). The volume of fluid (VOF) method enables the formation and destruction of the fluid bubble, its interaction with solid surfaces, and the transient of jets. Spherical particles having different diameters, free surface interaction, and densities can also be introduced in the VOF method.

Governing equations

The governing mass continuity equation utilized by FLOW 3D (Yakhot and Orszag 1986) is given below:

$$V_F \frac{\partial \rho}{\partial t} + \frac{\partial}{\partial x} (\rho u A_x) + R \frac{\partial}{\partial y} (\rho u A_y) + \frac{\partial}{\partial z} (\rho w A_z) + C \frac{\rho u A_x}{x} = R_{DIF} + R_{SOR} \quad (\text{Yakhot and Orszag 1986}) \quad (1)$$

where

V_F	in the equation is the fractional volume.
u	is the flowing fluid velocity.
ρ	is the flowing fluid density.
R	in the equation represents the Reynolds number.
C	in the equation represents the constant of proportionality.
R_{DIF}	is known as the turbulent diffusion.

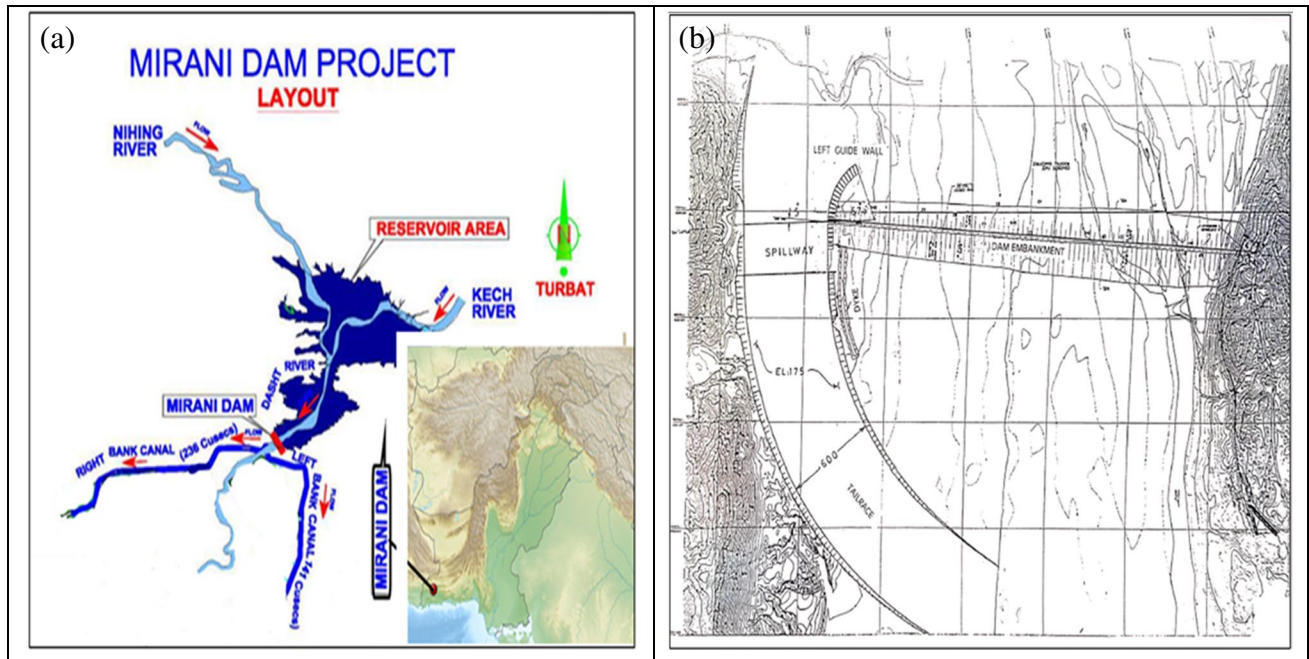


Fig. 1 a Layout and location of Mirani Dam. b Plan layout of Mirani Dam and spillway (adopted from WAPDA model studies cell, IRI Lahore, 2003)

Table 1 Salient features of Mirani Dam (adopted from WAPDA model studies cell physical model report, IRI Lahore, 2003)

Type	Concrete-faced rockfill dam
Crest level	86.5 m
Maximum height above the riverbed	38.7 m
Length of crest	964.6 m
Crest width	6.1 m
Slope U/S	1V to 1.6H
Slope D/S	1V to 1.6H

R_{SOR} is called mass source.

$A_x, A_y,$ and A_z in the equations represent the fractional areas in $x, y,$ and z directions individually.

The equations of motion (Versteeg and Malalasekera 1979) solved by FLOW 3D for the flowing fluid are given below:

$$\frac{\partial u}{\partial t} + \frac{1}{V_F} \left\{ uA_x \frac{\partial u}{\partial x} + vA_y R \frac{\partial u}{\partial y} + wA_z \frac{\partial u}{\partial z} \right\} - \xi \frac{A_y v^2}{xV_F} = -\frac{1}{\rho} \frac{\partial p}{\partial x} + G_x + f_x - b_x - \frac{R_{SOR}}{\rho V_F} (u - u_w - \delta u_s) \tag{2}$$

$$\frac{\partial v}{\partial t} + \frac{1}{V_F} \left\{ uA_x \frac{\partial v}{\partial x} + vA_y R \frac{\partial v}{\partial y} + wA_z \frac{\partial v}{\partial z} \right\} + \xi \frac{A_y uv}{xV_F} = -\frac{1}{\rho} R \frac{\partial p}{\partial y} + G_y + f_y - b_y - \frac{R_{SOR}}{\rho V_F} (v - v_w - \delta u_s) \tag{3}$$

$$\frac{\partial w}{\partial t} + \left\{ uA_x \frac{\partial w}{\partial x} + vA_y R \frac{\partial w}{\partial y} + wA_z \frac{\partial w}{\partial z} \right\} = -\frac{1}{\rho} \frac{\partial p}{\partial z} + G_z + f_z - b_z - \frac{R_{SOR}}{\rho V_F} (w - w_w - \delta w_s) \tag{4}$$

The effects of turbulence in turbulent flows are modeled using the equation for the specific kinetic energy with fluctuating flowing fluid velocity (Tabbara et al. 2005) which is given below:

$$K_T = \frac{1}{2} (u'^2 + v'^2 + w'^2) \tag{5}$$

where u', v', w' in the equation represents the flowing fluid velocity in the $x, y,$ and z directions.

The renormalization group (RNG) model is a more sophisticated version of the k -model (Chen et al. 2002; Yakhot and Orszag 1986). The equations for both models are the same. The RNG model renormalizes the Navier–Stokes equation to include the effect of small-scale motion. The difference between the two models is that the constants in the k -model are computed empirically, whereas the constants in the RNG model are

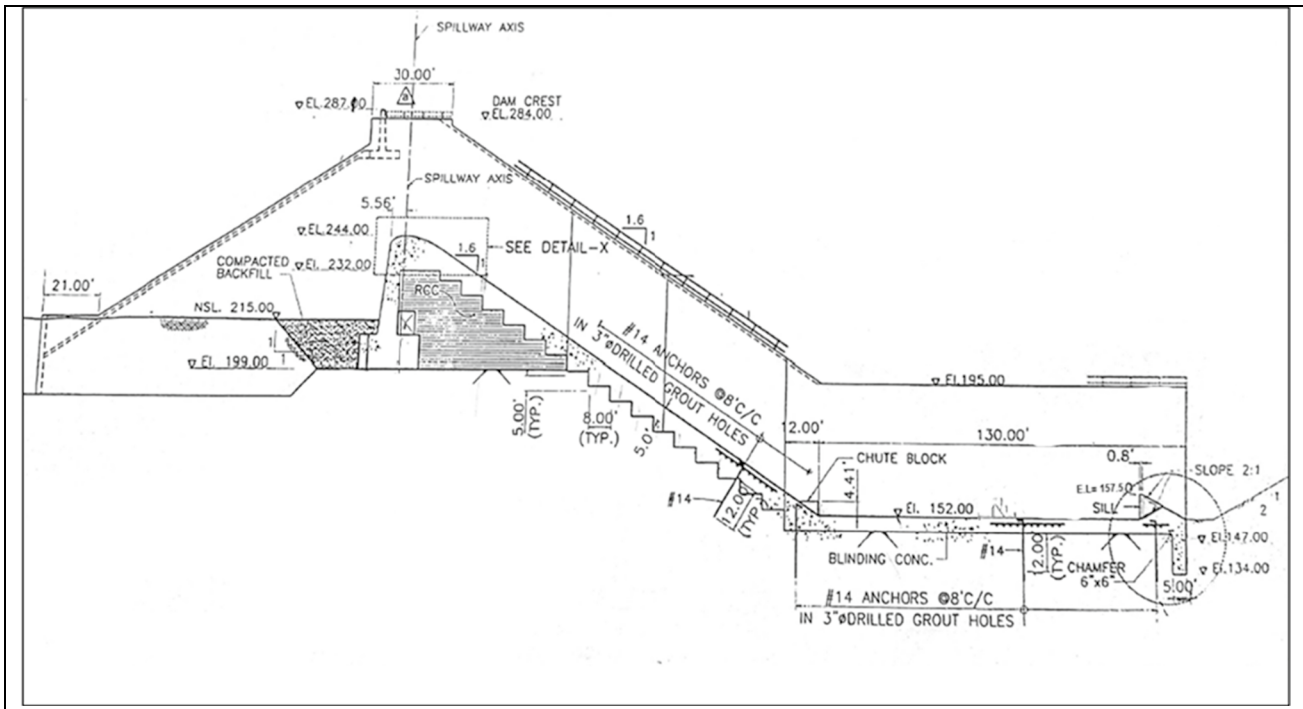
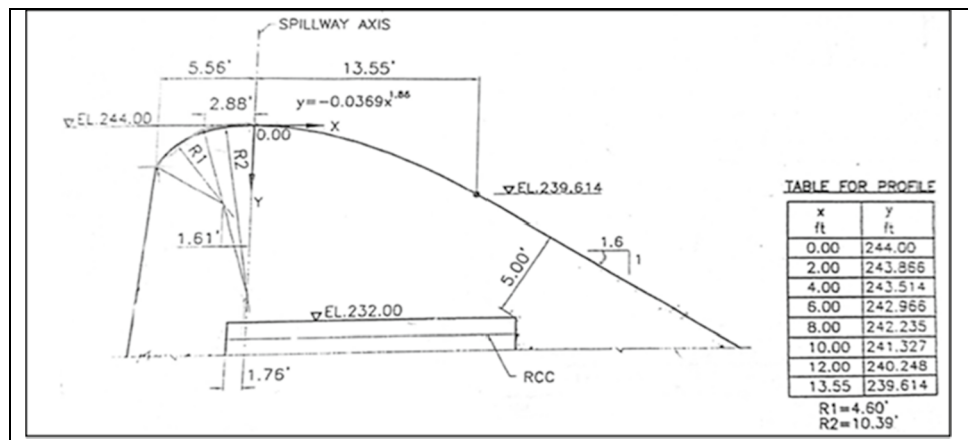


Fig. 2 Cross section of Mirani Dam spillway and USBR type III stilling basin (adopted from WAPDA model studies cell, IRI Lahore, 2003)

Fig. 3 Ogee profile of Mirani Dam spillway (adopted from WAPDA model studies cell, IRI Lahore, 2003)



computed explicitly. The RNG model is more accurate than the *k*-model. The small-scale intensity turbulent flows are delineated by the RNG model with good accuracy.

Methodological limitations

The study was carried out using the latest CFD-coded latest software package FLOW 3D, which increases the chances of the solver releasing errors and yield an unstable solution. Although good care was taken to carry out validation and follow the ASCE and ASME uncertainty and validation guidelines, still the possibility of a few numerical errors still

persists. Numerical approximations are always challenging and unpredictable (Sarkardeh et al. 2015). A numerical result may be distorted when trying for more accurate results (Frizell and Frizell 2015). In our study, careful attention to the mesh size, boundary conditions, and several physical parameters was given to get a proper and least errored simulation setup to make further simulations.

Data for Mirani Dam

Detailed engineering drawings of the Mirani Dam spillway and stilling basin were taken from the WAPDA Model

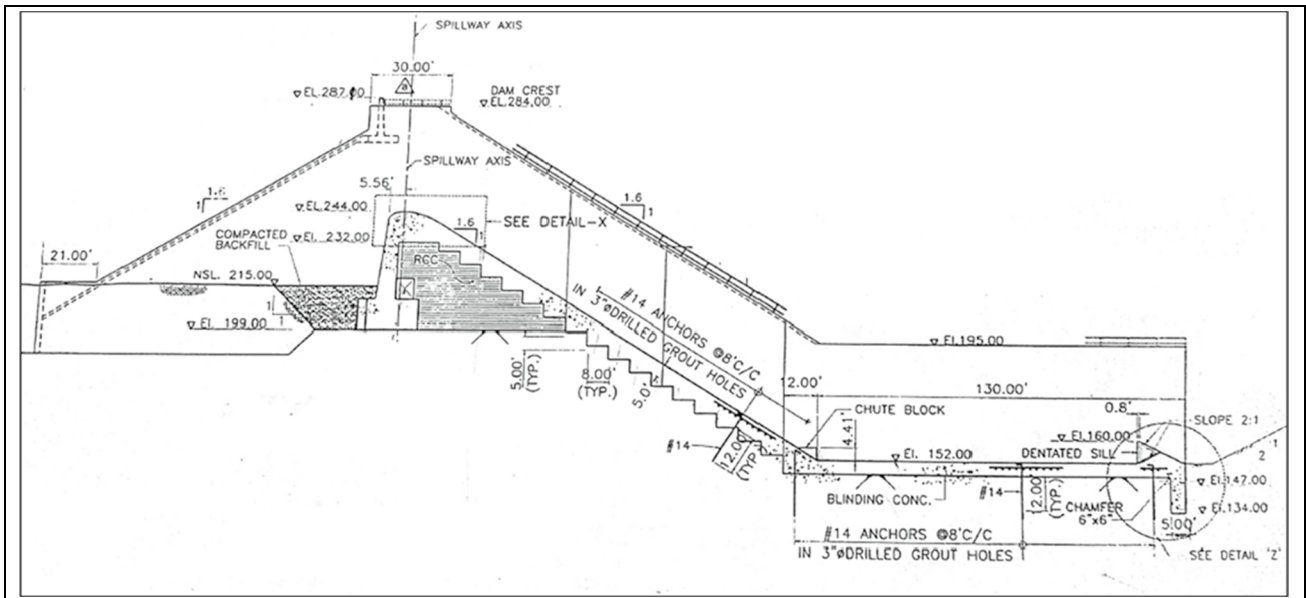


Fig. 4 Cross section of Mirani Dam spillway and USBR type II stilling basin (adopted from WAPDA model studies cell, IRI Lahore, 2003)

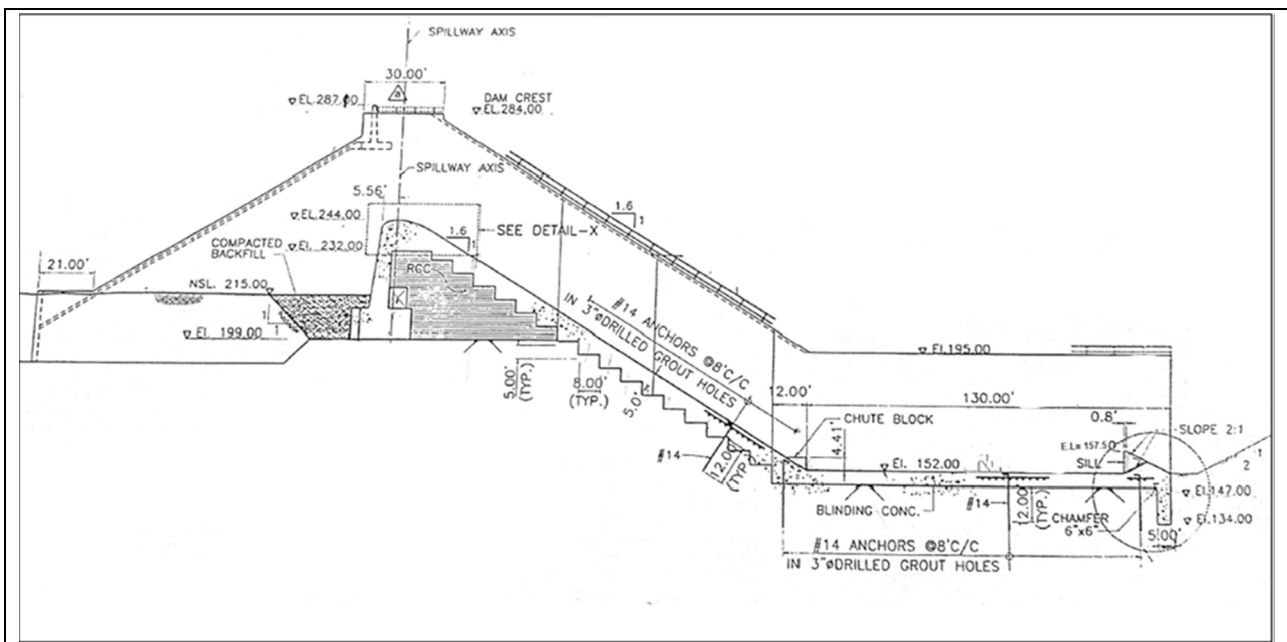


Fig. 5 Cross section of Mirani Dam spillway and USBR type III stilling basin (adopted from WAPDA model studies cell, IRI Lahore, 2003)

studies cell in the Irrigation Research Institute (IRI) Lahore. These drawings include dam and spillway cross sections. They are presented in Figs. 3, 4, and 5.

USBR type II stilling basin

The USBR type II stilling basin contains a chute block, stilling basin length, and dentated sill (Fig. 6). The dimensions

of these parts are given below. USBR type II stilling basin is presented in Fig. 7.

- Length of stilling basin = 39.5 m
- Height, width, and spacing of chute blocks = 1.35 m
- Height of dentated sill = 2.34 m
- Width of dentated sill = spacing of dentated sill = 1.83 m
- Top thickness of dentated sill = 0.3 m

Fig. 6 Baffle blocks dimension of USBR Type III stilling basin (Adopted from WAPDA model studies cell, IRI Lahore, 2003)

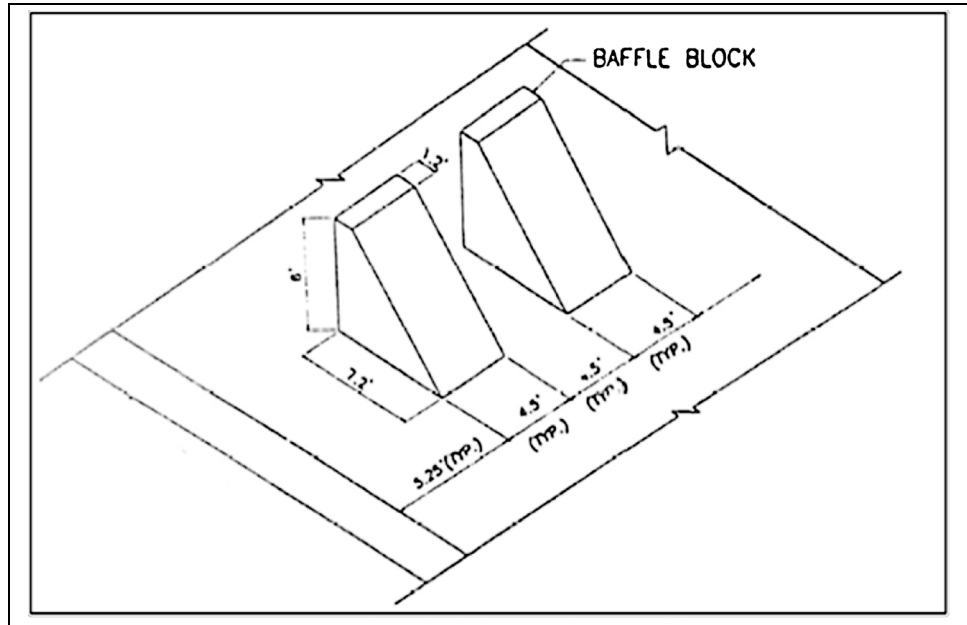
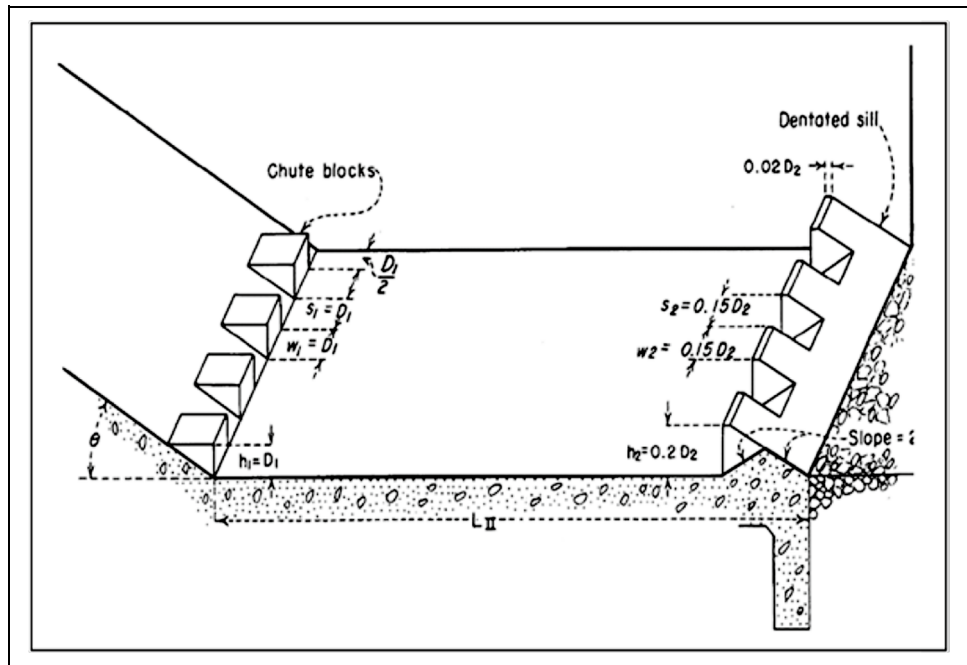


Fig. 7 USBR type II stilling basin typical dimensions from Paterka guide



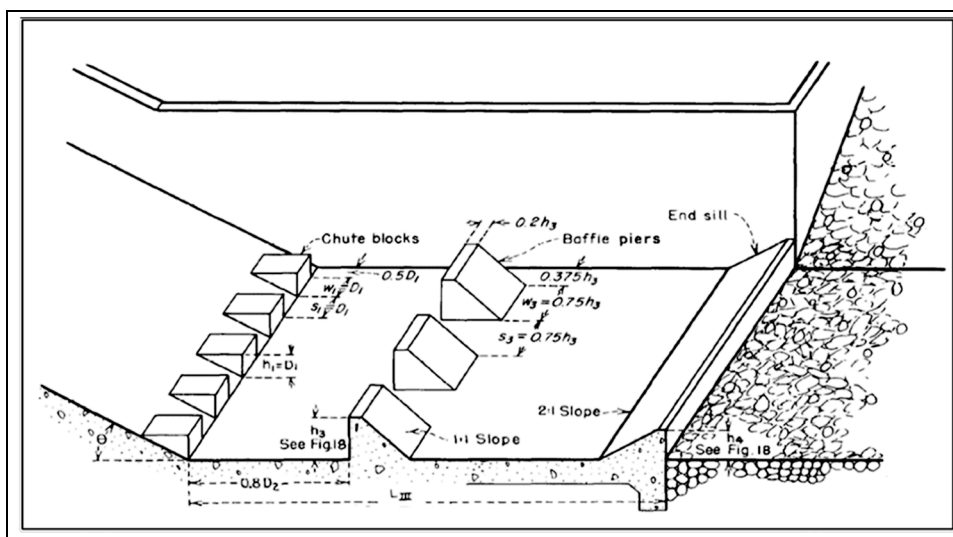
USBR type III stilling basin

USBR type III stilling basin contains chute blocks, stilling basin length, and a dentated sill. The dimensions of these parts are given below. USBR type III stilling basin is presented in Fig. 8.

- Length of stilling basin = 39.5 m
- Height, width, and spacing of chute blocks = 1.35 m

- Height of friction block = 1.8 m
- Width of friction block = Spacing of friction block = 1.37 m
- Top thickness of friction block = 0.36 m
- Slope of friction block = 1:1
- Height of end sill = 1.7 m
- Top thickness of end sill = 0.3 m
- Slope of end sill = 2:1

Fig. 8 USBR type III stilling basin typical dimensions from Paterka guide



General simulation setup

Five numerical models of the Mirani Dam spillway with a stilling basin were prepared, and the models were simulated in FLOW 3D by using their specific boundary conditions. The STL (stereolithography) 3D file as presented in Fig. 9 of the models was imported to FLOW 3D. The Numerical solver FLOW 3D can import 3D files from SOLIDWORKS to begin the simulation. To account for the turbulence in the flow due to the presence of steps, the RNG $k-\epsilon$ model was adopted. Different sub-models, such as the VOF model, to capture the free surface; air entrainment model, to capture the formation of bubbles in the flow due to air; density evaluation model, to address the variation in density of the water; and drift flux model, to cope with the formation of phase drag, were selected to create a virtual environment (Peng et al. 2019). Mesh sizes were adopted in a way to effectively capture all the features of geometry and free surface (Saqib et al. 2022b). A grid sensitivity analysis was

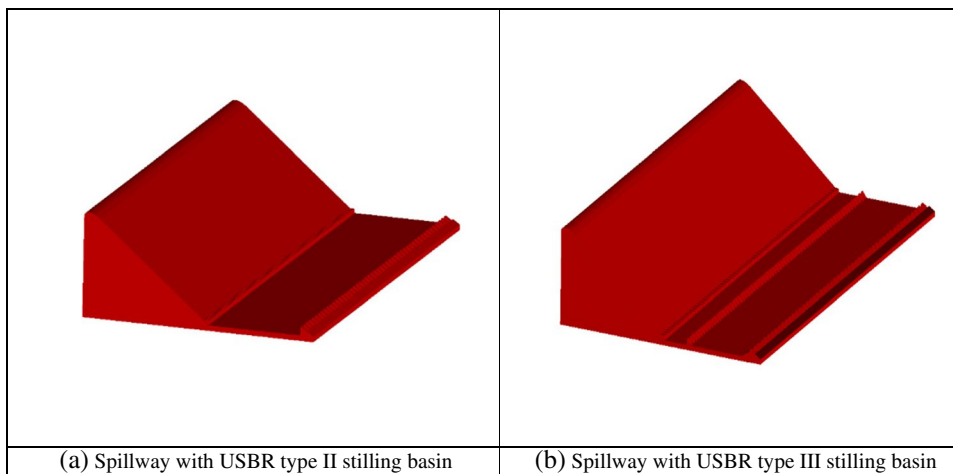
performed to get the most accurate results. In addition, fine mesh was avoided, keeping in view the computing power.

Mesh selection criterion

Four different mesh sizes, i.e., 2.3 m, 1.7 m, 1.3 m, and 0.9 m, were selected for the validation model and *GCI* (Grid Convergence Index) was employed to choose the effective mesh size. *GCI* is the effective method that is recommended by several researchers (Abbasi et al. 2021; Ghaderi et al. 2020; Ghaderi and Abbasi 2021). Here, the mesh refinement ratio ($r = G_{coarse}/G_{fine}$) is greater than 1.3 as recommended by Celik et al. (2008).

Just one parameter, which is average water elevation along the spillway physical model, was selected from the physical model results. The physical model was constructed at Nandipur Research Center, Lahore, Pakistan, and the results for the flow rate of $Q = 6032.2 \text{ m}^3/\text{s}$ were adopted for model validation. The apparent order of convergence can be calculated from the following expression (Boes and Hager 2003):

Fig. 9 STL geometry of Mirani Dam spillway



$$p = \ln \frac{f_3 - f_2}{f_2 - f_1} / \ln(r) \quad (\text{Boes and Hager 2003}) \quad (6)$$

Here, r is a refinement rate that is greater than in our case, and f_1 corresponds to the values of water elevation at the fine mesh. Similarly, f_2 and f_3 related to the values at medium and coarse mesh, respectively. The GCI for the fine grid is given below.

$$GCI_{32} = \frac{1.25 \left| \frac{f_3 - f_2}{f_2} \right|}{r^p - 1} \quad (\text{Abbasi et al. 2021}) \quad (7)$$

$$GCI_{12} = \frac{1.25 \left| \frac{f_2 - f_1}{f_1} \right|}{r^p - 1} \quad (\text{Celik et al. 2008}) \quad (8)$$

Here, the grid convergence is obtained. The grid parameters are calculated from the equations given above. GCI values for the finer grid came out to be smaller than the coarser grids. It is, therefore, inferred that no further mesh refinement is required. According to ASME (2008), ASCE (2009), and Ghaderi and Abbasi (2021), if the value of the $GCI_{23}/r^p GCI_{12}$ is closer to one, then the solutions are in the asymptotic range of convergence. Hence, the mesh size of 0.9 m was chosen to be effective for our study, as shown in the following Fig. 10.

Boundary conditions selection criterion

The importance of boundary conditions in a simulation cannot be overstated. The sort of boundary conditions used on the boundaries has a considerable impact on the results. Here, the ASME (2008) and ASCE (2009) guidelines were followed, and the least errored combination of boundary conditions was selected. The following sets of boundary conditions were tested on the validation model, i.e., spillway with USBR type II stilling basin.

Table 2 displays the different boundary conditions adopted for the validation. The sensitivity analysis has been carried out utilizing three sets of boundary conditions for a flow rate of 283.4 m³/s. The comparison of average water levels for different boundary conditions scenarios at a discharge of 283.4 m³/s is shown in Table 4. The set 2 boundary conditions scenario is utilized in research simulation due to good agreement with physical model results also displayed in Fig. 11. The model results are reported in the “Results” section.

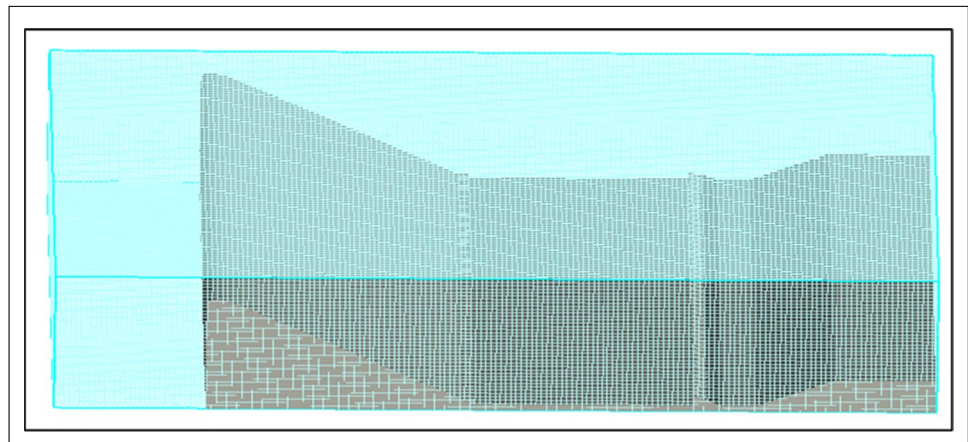
Results and discussion

The present section contains two major parts. One part is related to model validation and calibration, while the other is related to the selection of a better energy dissipator based on the velocity profile, energy dissipation, and flow elevation.

Table 2 Boundary conditions sensitivity analysis

(A) Set 1			
X_{min}	Specified pressure	X_{max}	Specified pressure
Y_{min}	Wall	Y_{max}	Wall
Z_{min}	Wall	Z_{max}	Specified pressure
(B) Set 2			
X_{min}	Volume flow rate	X_{max}	Specified wall
Y_{min}	Wall	Y_{max}	Wall
Z_{min}	Wall	Z_{max}	Specified wall
(C) Set 3			
X_{min}	Volume flow rate	X_{max}	Outflow
Y_{min}	Wall	Y_{max}	Wall
Z_{min}	Wall	Z_{max}	Specified wall

Fig. 10 Meshing adopted for validation and calibration (spillway with USBR type II stilling basin)



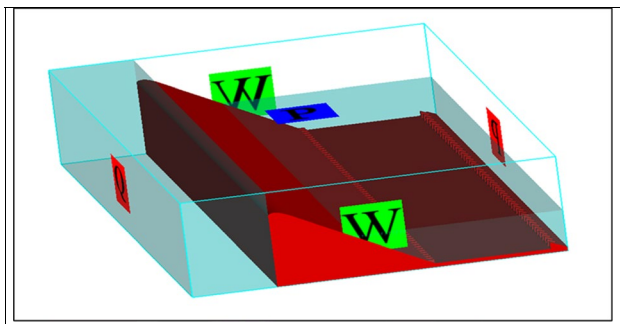


Fig. 11 Boundary conditions set 2 adopted for validation model and further simulations

Model validation and calibration results

As discussed earlier, grid sensitivity and boundary condition sensitivity analyses were done to get the specific conditions for the least error simulation. The following tables present the average water surface elevation along the spillway length when the different mesh sizes and boundary conditions were employed in a simulation. As discussed earlier, three mesh sizes of 0.9 m, 1.3 m, 1.7 m, and 2.3 m, respectively, were used in the free-flow simulation of the model. The comparison of the average water level numerically computed and physically observed along the Mirani Dam spillway and stilling basin with different mesh sizes at $Q = 6032.2 \text{ m}^3/\text{s}$ is shown in the following Table 3. The simulation with 0.9-m uniform mesh predicted water depth accurately along the spillway and stilling basin as compared to other mesh sizes. The uniform mesh size of 0.9 m was adopted for further research and simulations.

The boundary condition sensitivity analysis was carried out using three sets of boundary conditions at a discharge of $283.4 \text{ m}^3/\text{s}$. The comparison of average water levels for different boundary conditions scenarios at a discharge of $283.4 \text{ m}^3/\text{s}$ is given in Table 4. The set 2 boundary conditions scenario is utilized in further simulations due to good agreement with physical model results.

Table 3 Comparison of average water level at different mesh sizes ($Q = 6032.2 \text{ m}^3/\text{s}$)

Sr no.	Mesh size (m)	Average physically observed water level (m)	Average numerically computed water level (m)	Error (%)
1	2.3	62.4	68.7	6.3
2	1.7	62.4	65.4	3
3	1.3	62.4	64	1.7
4	0.9	62.4	62.7	0.3

Table 4 Comparison of average water levels for different boundary conditions scenario

Description	Average physically observed water level (m)	Average numerically computed water level (m)	Error (%)
Set 1	60.7	61.2	0.8
Set 2	60.7	61.1	0.7
Set 3	60.7	61.4	1.2

Stilling basin performance evaluation

Five types of stilling basins were selected for the simulation in FLOW 3D to look for the optimized energy dissipator. (1) USBR type II stilling basin with a floor length of 39.5 m, (2) USBR type II stilling basin with a floor length of 44.2 m, (3) USBR type II stilling basin with a floor length of 48.8 m, (4) USBR type III stilling basin with a floor length of 39.5 m, and (5) USBR type III stilling basin. The block height increased by 0.3 m. Each of the five choices was analyzed to explore the best energy dissipator and least expensive alternative.

USBR type II stilling basin with 39.5-m floor length

In this case, the stilling basin is 39.5 m in length with a 1.35-m-high chute blocking the upstream of a 2.34-m-high dentated sill at the tail end. The simulations were performed as discussed earlier in “General simulation setup” section. This selection was subjected to two flow rates: $6032.2 \text{ m}^3/\text{s}$ (200-year return period) and $11,954.4 \text{ m}^3/\text{s}$ (PMF). Three parameters, water surface elevation, specific energy, and velocity profiles, were made from FLOW 3D with the help of FLOW Sight. They are presented in Figs. 12 and 13.

It can be seen from Figs. 12 and 13 that the hydraulic jump of $6032.2 \text{ m}^3/\text{s}$ has been well contained toward the stilling basin as compared to the flow rate of $11,954.4 \text{ m}^3/\text{s}$. This option replicates the less effective way as the hydraulic jump has been moved over the spillway. The velocity and specific energy at the start of the jump are 19 m/s and 19.8 m, respectively, which after dissipation are reduced to 5.3 m/s and 9.1 m, respectively. Similarly, at a flow rate of $11,954.4 \text{ m}^3/\text{s}$, the hydraulic jump has been swept out of the stilling basin. The velocity and specific energy at the start of the jump are 22.7 m/s and 28.9 m, respectively, which after dissipation are reduced to 6.7 m/s and 12.2 m, respectively.

USBR type II stilling basin with 44.2-m floor length

Here, the length of stilling basin is equal to 44.2 m, a different option for the spillway of Mirani Dam. As discussed earlier, two major flow rates that are $6032.2 \text{ m}^3/\text{s}$ and $11,954.4 \text{ m}^3/\text{s}$ were simulated in FLOW 3D to present the

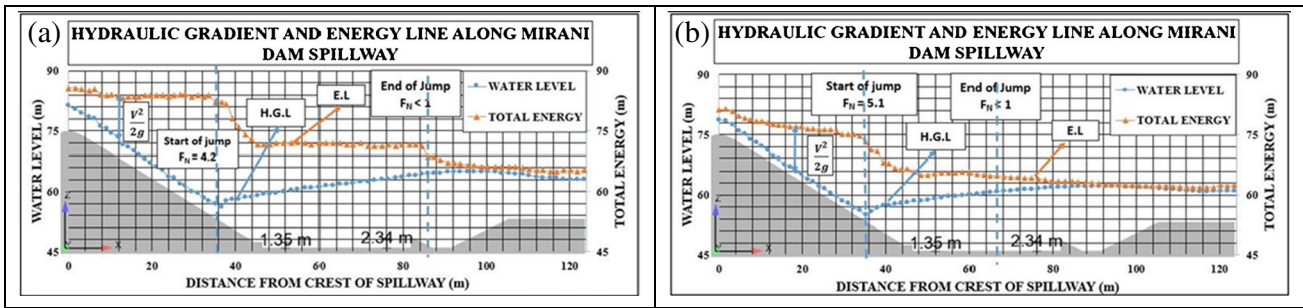


Fig. 12 a Water surface and specific energy profile of USBR type II stilling basin with 39.5-m floor length for the discharge of 6032.2 m³/s. b Water surface and specific energy profile of USBR type II stilling basin with 39.5-m floor length for the discharge of 11,954.4 m³/s

Fig. 13 a Velocity profile along spillway and USBR type II stilling basin with 39.5-m floor length for the discharge of 6032.2 m³/s. b Velocity profile along spillway and USBR type II stilling basin with 39.5-m floor length for the discharge of 11,954.4 m³/s

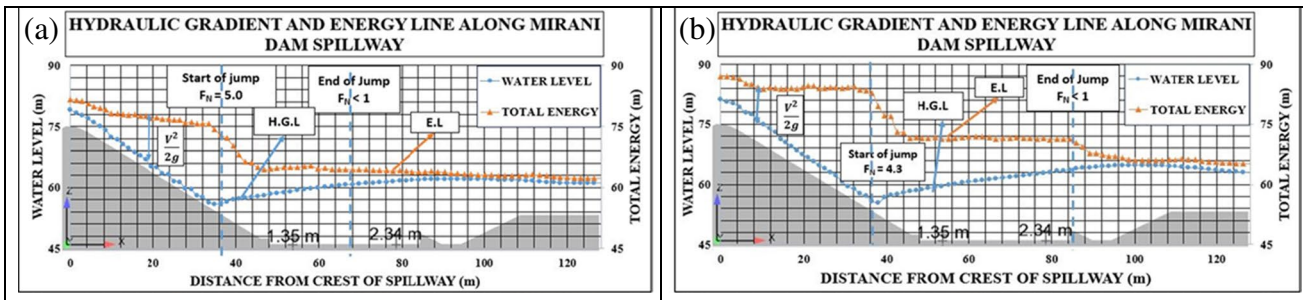
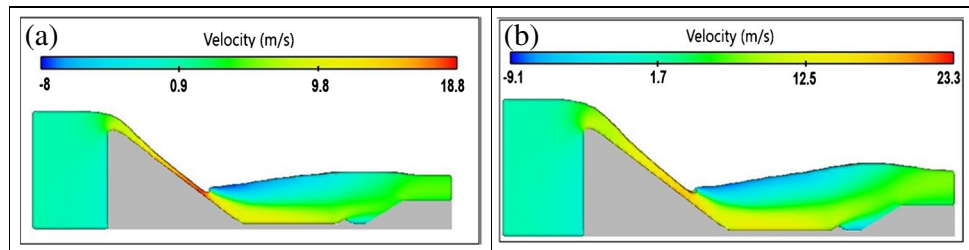
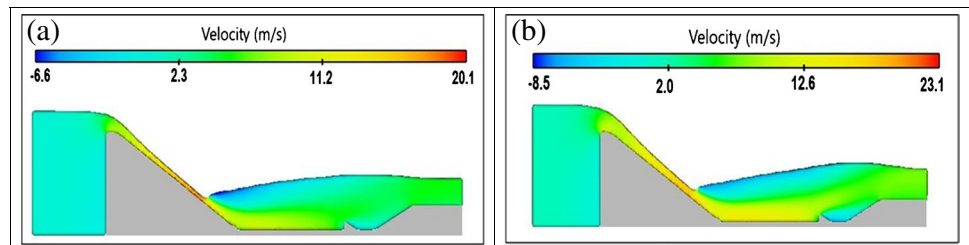


Fig. 14 a Water surface and specific energy profile of USBR type II stilling basin with 44.2-m floor length for the discharge of 6032.2 m³/s. b Water surface and specific energy profile of USBR type II stilling basin with 44.2-m floor length for the discharge of 11,954.4 m³/s

Fig. 15 a Velocity profile along spillway and USBR type II stilling basin with 44.2-m floor length for the discharge of 6032.2 m³/s. b Velocity profile along spillway and USBR type II stilling basin with 44.2-m floor length for the discharge of 11,954.4 m³/s



water surface, specific energy, and velocity profile along the spillway. This is shown in Figs. 14 and 15. Figures 14 and 15 present the water surface profiles, specific energy surface profiles, and velocity profiles for the flow rates of 6032 m³/s and 11,954.4 m³/s, respectively, for the USBR type II stilling basin for 44.2-m floor length. It can be seen

that the hydraulic jump at 6032.2 m³/s has been well contained toward the stilling basin. The velocity and specific energy at the start of the jump are 19.5 m/s and 20.3 m, respectively, which after dissipation are reduced to 4.9 m/s and 8.9 m, respectively. Therefore, it can be inferred that as compared to 1st, this option is more effective. Similarly,

at the discharge of 11,954.4 m³/s, the hydraulic jump still extends beyond the sill of the stilling basin. The velocity and specific energy at the start of the jump are 23 m/s and 29.8 m, respectively, which after dissipation are reduced to 6.3 m/s and 12 m, respectively. In comparison to the 1st option, they are slightly less.

USBR type II stilling basin with 48.4-m floor length

The same geometry with a longer stilling basin of 48.8 m presents the third option. From Figs. 16 and 17, it is evident that the hydraulic jump at 6032.2 m³/s has been well contained inside the stilling basin. The velocity and specific energy at the start of the jump are 19.2 m/s and 20.4 m, respectively, which after dissipation are reduced to 4.4 m/s and 8.6 m, respectively. Similarly, at a discharge of 11,954.4 m³/s, the hydraulic jump is well contained within the stilling basin. The velocity and specific energy at the start of the jump are 22.9 m/s and 30 m, respectively, which after dissipation are reduced to 5.3 m/s and 11.1 m, respectively. When compared to the first two options, this option looks better as residual velocity is less at the end.

USBR type III stilling basin with 39.5-m floor length

This option contains USBR type III stilling basin with 1.3-m chute block, 1.8-m-high baffle blocks, and 1-m-high solid sloping end sill. Same discharge values of 200-year return period and PMF were used to simulate the flow over this option.

Figures 18 and 19 present the water surface profiles, specific energy surface profiles, and velocity profiles for the USBR type III stilling basin for 39.5-m floor length. It is evident from the figures that the hydraulic jump at 6032.2 m³/s has been well contained inside the stilling basin. The velocity and specific energy at the start of the jump are 19.5 m/s and 21.3 m, respectively, which after dissipation are reduced to 4.3 m/s and 8.5 m, respectively. In addition to this, at the discharge of 11,954.4 m³/s, the hydraulic jump is also well contained within USBR type III stilling basin having 39.5-m length. The baffle blocks minimized the length of the stilling basin to contain hydraulic jump as compared to USBR type II stilling basin. The velocity and specific energy at the start of the jump are 23 m/s and 30.1 m, respectively, which after dissipation are reduced to 6 m/s and 11.3 m, respectively.

USBR type III stilling basin with chute and friction blocks height increased by 0.3 m

The chute and baffle block of the previously adopted 4th model (option) with USBR type III stilling basin is increased in height by 0.3 m, whereas stilling basin length and the height of end sill has remained the same as in the previous model with USBR type III stilling basin. With the same flow rates, water surface profile and velocity profile are shown in Figs. 20 and 21.

It is evident from Fig. 21 that the hydraulic jump at 6032.2 m³/s has been well contained inside the stilling basin. The velocity and specific energy at the start of the jump are 19.5 m/s and 20.8 m, respectively, which after dissipation

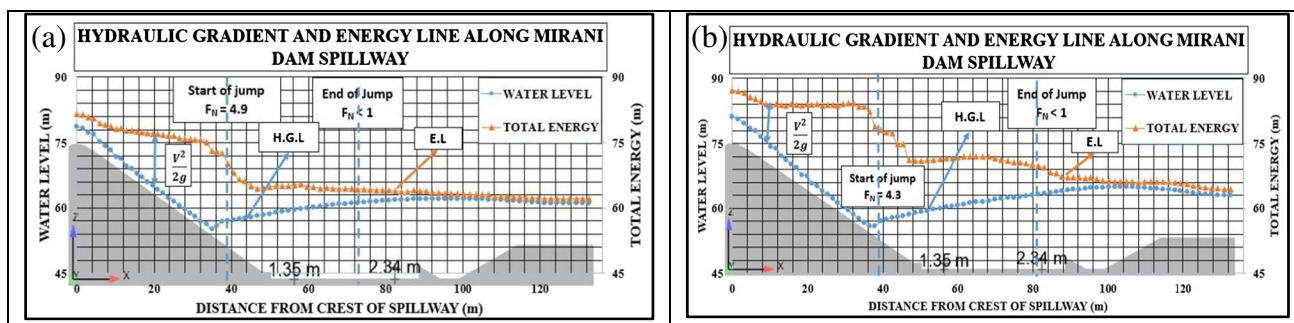
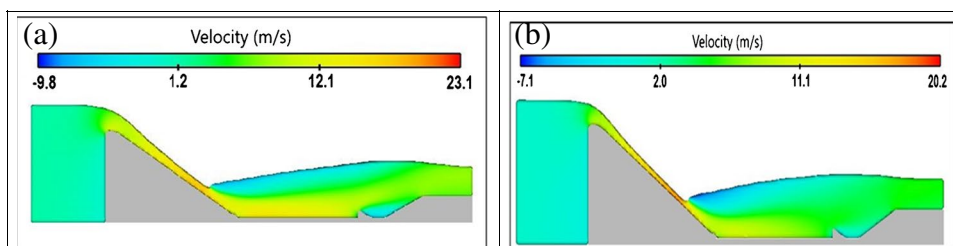


Fig. 16 a Water surface and specific energy profile of USBR type II stilling basin with 48.4-m floor length for the discharge of 6032.2 m³/s. b Water surface and specific energy profile of USBR type II stilling basin with 48.4-m floor length for the discharge of 11,954.4 m³/s

Fig. 17 a Velocity profile along spillway and USBR type II stilling basin with 48.4-m floor length for the discharge of 6032.2 m³/s. b Velocity profile along spillway and USBR type II stilling basin with 48.4-m floor length for the discharge of 11,954.4 m³/s



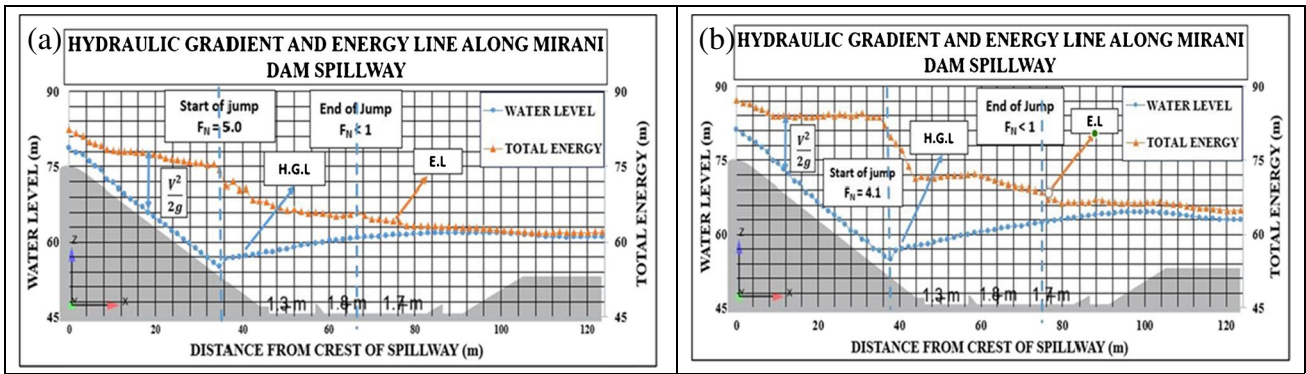


Fig. 18 a Water surface and specific energy profile of USBR type III stilling basin with 39.5-m floor length for the discharge of 6032.2 m³/s. b Water surface and specific energy profile of USBR type III stilling basin with 39.5 m floor length for the discharge of 11,954.4 m³/s

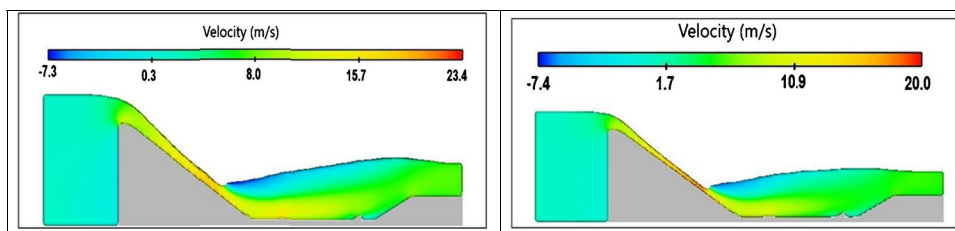


Fig. 19 a Velocity profile along spillway and USBR type III stilling basin with 39.5-m floor length for the discharge of 6032.2 m³/s. b Velocity profile along spillway and USBR type III stilling basin with 39.5-m floor length for the discharge of 11,954.4 m³/s

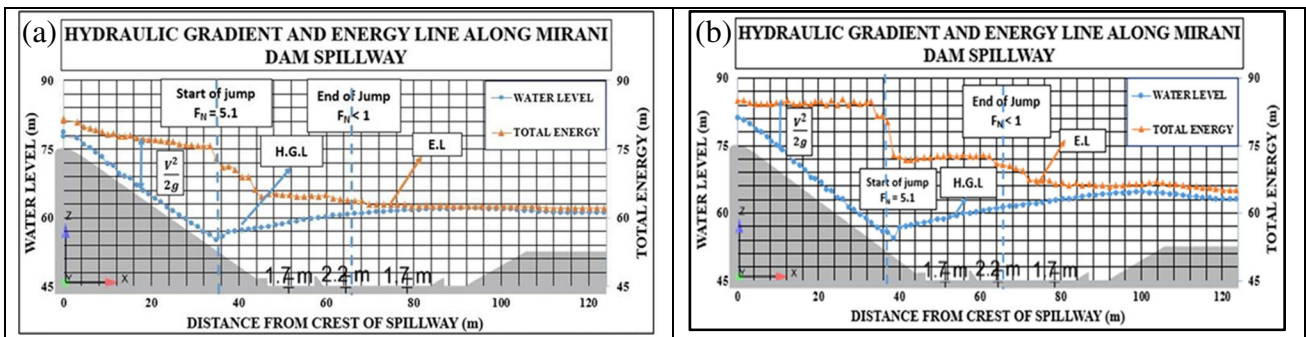


Fig. 20 a Water surface and specific energy profile of USBR type III stilling basin with chute and friction blocks height increased by 0.3 m with 39.5-m floor length for the discharge of 6032.2 m³/s. b Water

surface and specific energy profile of USBR type III stilling basin with chute and friction blocks height increased by 0.3 m stilling basin with 39.5-m floor length for the discharge of 11,954.4 m³/s

are reduced to 4.3 m/s and 8.7 m, respectively. The increased dimensions of chute and baffle blocks result in a negligible reduction in velocity. Similarly, at the discharge of 11,954.4 m³/s, the hydraulic jump is also well contained inside the USBR type III stilling basin having 39.5-m floor length. The velocity and specific energy at the start of the jump are 23 m/s and 30.2 m, respectively, which after dissipation are reduced to 6.2 m/s and 11.6 m, respectively.

Cost analysis of the different types of stilling basins

The economic analysis takes into account the costs of earthwork, concrete, and reinforcing steel. The quantities required for the construction of the Mirani Dam spillway were calculated, and the total cost was determined by multiplying these quantities by the unit rates. The unit rates

were derived from the Government of Baluchistan's Composite Schedule of Rates, Version 2018. The earthwork estimation was done by obtaining the natural surface level along the Mirani Dam spillway and stilling basin from the GTOPO30 DEM (Digital Elevation Model) using ArcGIS. The mid-sectional area method and mean sectional area method were used to estimate earthwork quantity. Tables 5, 6, 7, 8, 9, and 10 present the cost analysis for each type of stilling basin. The total estimate to build the dam is presented at the end.

Selecting the best stilling basin/energy dissipator

The satisfactory performance of the stilling basin relies on many factors involved in the dissipation operation. The choice of stilling basin in this research has been made on the following four factors: (1) magnitude of downstream velocity, (2) magnitude of energy dissipation, (3) turbulent kinetic energy, and (4) total cost (Güven and Mahmood 2021). The hydraulic jump at the discharge of 11,954.4 m³/s has been swept out of the USBR type II stilling basin with 39.5 m and

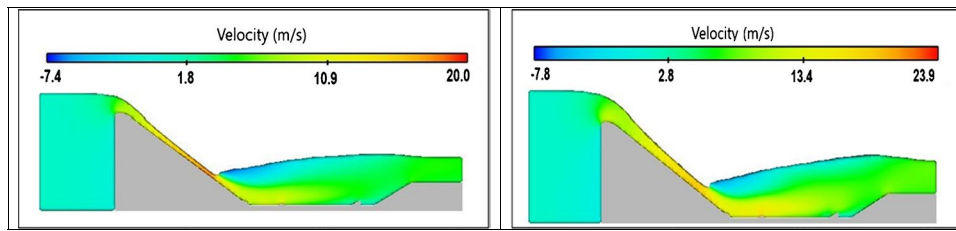


Fig. 21 a Velocity profile along spillway and USBR type III stilling basin with chute and friction block height increased by 0.3 m with 39.5-m floor length for the discharge of 6032.2 m³/s. **b** Velocity profile

along spillway and USBR type III stilling basin with chute and friction block height increased by 0.3 m with 39.5-m floor length for the discharge of 11,954.4 m³/s

Table 5 Estimation of Mirani Dam spillway and USBR type II basin with 39.5-m floor length

Sr. no.	Description	Length m	Cross-sectional area m ²	Number	Quantity m ³	Remarks
1	Earth work	–	–	–	237,301.9	–
2	Ogee spillway	182.9	206.2	–	37,726.4	M20
3	Chute	182.9	66.2	–	12,108.1	M20
4	Stilling basin floor	182.9	60.4	–	11,052.1	M20
5	Chute block	1.3	1.4	68.0	132.4	M20
6	Dentated sill	182.9	6.6	–	1200.8	M20
7	Steel reinforcement	182.9	0.7	–	121.8	Grade 40
Total cost					827,039,616	Rupees

Table 6 Estimation of Mirani Dam spillway and USBR type II basin with 44.2-m floor length

Sr. no.	Description	Length m	Cross-sectional area m ²	Number	Quantity m ³	Remarks
1	Earth work	–	–	–	255,191.8	–
1	Ogee spillway	182.9	206.2	–	37,726.4	M20
2	Chute	182.9	66.2	–	12,108.1	M20
3	Stilling basin floor	182.9	67.4	–	12,327.3	M20
4	Chute block	1.3	1.4	68.0	132.4	M20
5	Dentated sill	182.9	6.6	–	1200.8	M20
6	Steel reinforcement	182.9	0.7	–	124.3	Grade 40
Total cost					845,342,617	Rupees

Table 7 Estimation of Mirani Dam spillway and USBR type II basin with 48.8-m floor length

Sr. no.	Description	Length m	Cross-sectional area m ²	Number	Quantity m ³	Remarks
1	Earth work	–	–	–	271,993.7	–
1	Ogee spillway	182.9	206.2	–	37,726.4	M20
2	Chute	182.9	66.2	–	12,108.1	M20
3	Stilling basin floor	182.9	74.4	–	13,602.5	M20
4	Chute block	1.3	1.4	68.0	132.4	M20
5	Dentated sill	182.9	6.6	–	1200.8	M20
6	Steel reinforcement	182.9	0.7	–	126.9	Grade 40
Total cost					863,536,812	Rupees

Table 8 Estimation of Mirani Dam spillway and USBR type III basin with 39.5-m floor length

Sr. no.	Description	Length m	Cross-sectional area m ²	Number	Quantity m ³	Remarks
1	Earth work	–	–	–	237,301.9	–
1	Ogee spillway	182.9	206.2	–	37,726.4	M20
2	Chute	182.9	66.2	–	12,108.1	M20
3	Stilling basin floor	182.9	60.4	–	11,052.1	M20
4	Chute block	1.3	1.4	68.0	132.4	M20
5	Friction block	2.2	2.3	66.0	339.4	M20
6	Solid end sill	182.9	3.1	–	564.5	M20
7	Steel reinforcement	182.9	0.7	–	121.8	Grade 40
Total cost					823,733,842	Rupees

Table 9 Estimation of Mirani Dam spillway and USBR type III stilling basin with a 0.3-m increase in height of chute and baffle blocks having 39.5-m floor length

Sr. no.	Description	Length m	Cross-sectional area m ²	Number	Quantity m ³	Remarks
1	Earth work	–	–	–	237,301.9	–
1	Ogee spillway	182.9	206.2	–	37,726.4	M20
2	Chute	182.9	66.2	–	12,108.1	M20
3	Stilling basin floor	182.9	60.4	–	11,052.1	M20
4	Chute block	1.3	2.1	68.0	192.5	M20
5	Friction block	2.2	2.7	66.0	396.8	M20
6	Solid end sill	182.9	3.1	–	564.5	M20
7	Steel reinforcement	182.9	0.7	–	121.8	Grade 40
Total cost					825,041,979	Rupees

44.2 m. The other three alternatives all contain hydraulic jumps within the stilling basin. The comparison between these alternatives has been presented below in the following Table 10.

It is evident from the above table that the USBR type III stilling basin having 39.5-m length contained the hydraulic jump within the stilling basin and is the best option as compared to other alternatives based on hydraulics

and cost analysis. This is consistent with the studies performed by Asaram et al. (2016) and Herrera-Granados and Kostecki (2016) who also proposed the same type of USBR type III stilling basins with different lengths of stilling basins. This is because they performed studies on different dam sites.

To develop more confidence, the energy dissipation by all the abovementioned alternatives was compared with

Table 10 Comparison of performance and cost of stilling basin

Description	Discharge (m ³ /s)	U/S energy (m)	D/S energy (m)	Energy dissipation (%)	D/S velocity (m/s)	Cost (million PKR)
USBR type II (<i>L</i> = 48.8 m)	6032.2	20.4	8.6	58.1	4.4	0.86
	11,954.4	30.0	11.1	62.9	5.3	
USBR type III (<i>L</i> = 35.5 m)	6032.2	21.3	8.5	60.2	4.3	0.82
	11,954.4	30.1	11.3	62.3	6.0	
USBR type III with 0.3-m increments in blocks (<i>L</i> = 35.5 m)	6032.2	20.8	8.7	58.2	4.3	0.83
	11,954.4	30.2	11.6	61.7	6.2	

Table 11 Comparison of physical and numerical models of Mirani Dam spillway and stilling basin

Description	% Energy dissipation (FLOW 3D)	% Energy dissipation (physical)	% Difference
USBR type II (<i>L</i> = 48.8 m)	58.1	58.4	0.6
	62.9	65.4	3.9
USBR type III (<i>L</i> = 35.5 m)	60.2	57.9	3.7
	62.3	62.7	0.5
USBR type III with 0.3-m increments in blocks (<i>L</i> = 35.5 m)	58.2	56.3	3.3
	61.7	63.6	3.2

the numerical solver FLOW 3D values. Both the values showed good agreement as the error percentage was obtained to be less than 5%. This is obvious from Table 11.

Conclusion and policy recommendations

Conclusion

The present study proposed different energy dissipator options for Mirani Dam, Pakistan. As spillways and stilling basins serve as the energy dissipators in dams, five different options for stilling basins based on hydraulic performance and cost analysis were explored. To conduct the research, the latest CFD software, FLOW 3D, was used. Model validation was performed by comparing it with the magnitude of percentage dissipation of energies of each option with experimental values. The error range of 0–4% was obtained and the RMS Index was found to be less than 3. It was found that the USBR type III stilling basin, having a 39.5-m length, is the most satisfactory based on hydraulic and economic analyses. This stilling basin, when subjected to maximum flow rates of 6032.2 m³/s and 11,954.4 m³/s, contained the hydraulic jump within the stilling basin. The estimated cost of construction was found to be 0.82 million Pakistani rupees, the lowest of other basin options. Therefore, USBR type III

stilling basin, having a 39.5-m length, was proposed for construction.

Policy recommendations

The study was undertaken with the help of FLOW 3D, the latest CFD software package. Although the validation was done, due to the limitations of computational sources, error analysis was compromised (Saqib et al. 2021). A more involved and powerful validation can be performed when more computational power is available. The use of modern CFD software can be adopted as the best method to analyze and design hydraulic structures. In Pakistan, the use of CFD software is relatively limited compared to other countries. The presented study can be a benchmark for researchers and managers to learn about the capabilities of CFD. As previously stated, several energy dissipation options for the Mirani Dam were developed. These options yielded the best energy dissipator based on both hydraulic and cost analysis. This can help designers and managers look for an optimized energy dissipator. Furthermore, it can enhance the designer's ability to look for more than one option for dam and spillway shapes. After analyzing the several options, numerical validation can be done in order to check the precision of the results.

Funding This paper was supported by the Second Tibetan Plateau Scientific Expedition and Research Program (STEP) (Grant No. 2019QZKK0902) and National Natural Science Foundation of China (Grant No. 42077275). It was also supported by the Youth Innovation Promotion Association of the Chinese Academy of Sciences (2018405).

Declarations

Conflict of interest The authors declare no competing interests.

References

- Abbasi S, Fatemi S, Ghaderi A, Di Francesco S (2021) The effect of geometric parameters of the antivortex on a triangular labyrinth side weir. *Water (Switzerland)* 13(1). <https://doi.org/10.3390/w13010014>
- Amorim JCC, Amante RCR, Barbosa VD (2015) Experimental and numerical modeling of flow in a stilling basin. *Proceedings of the 36th IAHR World Congress 28 June–3 July, the Hague, the Netherlands, 1*, 1–6
- Asaram D, Deepamkar G, Singh G, Vishal K, Akshay K (2016) Energy dissipation by using different slopes of ogee spillway. *Int J Eng Res Gen Sci* 4(3):18–22
- Boes RM, Hager WH (2003) Hydraulic design of stepped spillways. *J Hydraul Eng* 129(9):671–679. [https://doi.org/10.1061/\(ASCE\)0733-9429\(2003\)129:9\(671\)](https://doi.org/10.1061/(ASCE)0733-9429(2003)129:9(671))
- Celik IB, Ghia U, Roache PJ, Freitas CJ, Coleman H, Raad PE (2008) Procedure for estimation and reporting of uncertainty due to discretization in CFD applications. *J Fluids Eng Trans ASME* 130(7):0780011–0780014. <https://doi.org/10.1115/1.2960953>
- Chen Q, Dai G, Liu H (2002) Volume of fluid model for turbulence numerical simulation of stepped spillway overflow. *J Hydraul Eng* 128(7):683–688. 10.1061/共ASCE天0733-9429共2002天128:7共683天CE
- Damiron R (2015) CFD modelling of dam spillway aerator. Lund University Sweden
- Dunlop SL, Willig IA, Paul GE (2016) Cabinet Gorge Dam spillway modifications for TDG abatement – design evolution and field performance. 6th International Symposium on Hydraulic Structures: Hydraulic Structures and Water System Management, ISHS 2016, 3650628160, 460–470. 10.15142/T3650628160853
- Fleit G, Baranya S, Bihs H (2018) CFD modeling of varied flow conditions over an ogee-weir. *Period Polytech Civ Eng* 62(1):26–32. <https://doi.org/10.3311/PPci.10821>
- Frizell KW, Frizell KH (2015) Guidelines for hydraulic design of stepped spillways. Hydraulic Laboratory Report HL-2015-06, May
- Ghaderi A, Abbasi S (2021) Experimental and numerical study of the effects of geometric appendage elements on energy dissipation over stepped spillway. *Water (Switzerland)* 13(7). <https://doi.org/10.3390/w13070957>
- Ghaderi A, Dasineh M, Aristodemo F, Ghahramanzadeh A (2020) Characteristics of free and submerged hydraulic jumps over different macroroughnesses. *J Hydroinform* 22(6):1554–1572. <https://doi.org/10.2166/HYDRO.2020.298>
- Güven A, Mahmood AH (2021) Numerical investigation of flow characteristics over stepped spillways. *Water Sci Technol Water Supply* 21(3):1344–1355. <https://doi.org/10.2166/ws.2020.283>
- Herrera-Granados O, Kostecki SW (2016) Numerical and physical modeling of water flow over the ogee weir of the new Niedów barrage. *J Hydrol Hydromech* 64(1):67–74. <https://doi.org/10.1515/johh-2016-0013>
- Ho DKH, Riddette KM (2010) Application of computational fluid dynamics to evaluate hydraulic performance of spillways in australia. *Aust J Civ Eng* 6(1):81–104. <https://doi.org/10.1080/14488353.2010.11463946>
- Kocaer Ö, Yazar A (2020) Experimental and numerical investigation of flow over ogee spillway. *Water Resour Manag* 34(13):3949–3965. <https://doi.org/10.1007/s11269-020-02558-9>
- Kumcu SY (2017) Investigation of flow over spillway modeling and comparison between experimental data and CFD analysis. *KSCE J Civ Eng* 21(3):994–1003. <https://doi.org/10.1007/s12205-016-1257-z>
- Li S, Li Q, Yang J (2019) CFD modelling of a stepped spillway with various step layouts. *Math Prob Eng* 2019:1–12. <https://doi.org/10.1155/2019/6215739>
- Muthukumaran N, Prince Arulraj G (2020) Experimental investigation on augmenting the discharge over ogee spillways with nanocement. *Civ Eng Archit* 8(5):838–845. <https://doi.org/10.13189/cea.2020.080511>
- Naderi V, Farsadizadeh D, Lin C, Gaskin S (2019) A 3D study of an air-core vortex using HSPIV and flow visualization. *Arab J Sci Eng* 44(10):8573–8584. <https://doi.org/10.1007/s13369-019-03764-3>
- Nangare PB, Kote AS (2017) Experimental investigation of an ogee stepped spillway with plain and slotted roller bucket for energy dissipation. *Int J Civ Eng Technol* 8(8):1549–1555
- Parsaie A, Moradinejad A, Haghiabi AH (2018) Numerical modeling of flow pattern in spillway approach channel. *Jordan J Civ Eng* 12(1):1–9
- Pasbani Khiavi M, Ali Ghorbani M, Yusefi M (2021) Numerical investigation of the energy dissipation process in stepped spillways using finite volume method. *J Irrig Water Eng* 11(4):22–37
- Peng Y, Zhang X, Yuan H, Li X, Xie C, Yang S, Bai Z (2019) Energy dissipation in stepped spillways with different horizontal face angles. *Energies* 12(23). <https://doi.org/10.3390/en12234469>
- Raza A, Wan W, Mehmood K (2021) Stepped spillway slope effect on air entrainment and inception point location. *Water (Switzerland)* 13(10). <https://doi.org/10.3390/w13101428>
- Reeve DE, Zuhaira AA, Karunarathna H (2019) Computational investigation of hydraulic performance variation with geometry in gabion stepped spillways. *Water Sci Eng* 12(1):62–72. <https://doi.org/10.1016/j.wse.2019.04.002>
- Rice CE, Kadavy KC (1996) Model study of a roller compacted concrete stepped spillway. *J Hydraul Eng* 122(6):292–297. [https://doi.org/10.1061/\(ASCE\)0733-9429\(1996\)122:6\(292\)](https://doi.org/10.1061/(ASCE)0733-9429(1996)122:6(292))
- Rong Y, Zhang T, Peng L, Feng P (2019) Three-dimensional numerical simulation of dam discharge and flood routing in Wudu reservoir. *Water (Switzerland)* 11(10). <https://doi.org/10.3390/w11102157>
- Saqib N, Akbar M, Pan H, Ou G, Mohsin M, Ali A, Amin A (2022) Numerical analysis of pressure profiles and energy dissipation across stepped spillways having curved risers. *Appl Sci* 12(448):1–18
- Saqib N, Ansari N, Babar M (2021) Analysis of pressure profiles and energy dissipation across stepped spillways having curved treads using computational fluid dynamics. *Intl Conf Adv Mech Eng* :1–10
- Saqib Nu, Akbar M, Huali P, Guoqiang O (2022) Numerical investigation of pressure profiles and energy dissipation across the stepped spillway having curved treads using FLOW 3D. *Arab J Geosci* 15(1):1363–1400. <https://doi.org/10.1007/s12517-022-10505-8>
- Sarkardeh H, Marosi M, Roshan R (2015) Stepped spillway optimization through numerical and physical modeling. *Int J Energy Environ* 6(6):597–606
- Serafeim A, Avgeris V, Hrissanthou V (2015) Experimental and numerical modeling of flow over a spillway. *Eur Water Publ* 14(2015):55–59. <https://doi.org/10.15224/978-1-63248-042-2-11>

- Sorensen RM (1986) Stepped spillway model investigation. *J Hydraul Eng* 112(12):1461–1472. <https://ascelibrary.org/doi/full/10.1061/%28ASCE%290733->
- Tabbara M, Chatila J, Awwad R (2005) Computational simulation of flow over stepped spillways. *Comput Struct* 83(27):2215–2224. <https://doi.org/10.1016/j.compstruc.2005.04.005>
- Valero D, Bung DB, Crookston BM, Matos J (2016) Numerical investigation of USBR type III stilling basin performance downstream of smooth and stepped spillways. 6th International Symposium on Hydraulic Structures: Hydraulic Structures and Water System Management, ISHS 2016, 3406281608, 635–646. <https://doi.org/10.15142/T340628160853>
- Versteeg H, Malalasekera W (1979) An introduction to computational fluid mechanics. (Vol. 2). [https://doi.org/10.1016/0010-4655\(80\)90010-7](https://doi.org/10.1016/0010-4655(80)90010-7)
- WAPDA model studies cell, IRI Lahore (2003) Mirani Dam Project hydraulic model studies for the spillway. November 2003
- Yakhot V, Orszag S (1986) Renormalization group analysis of turbulence. I. Basic theory. *J Sci Comput* 1(1):3–51

Springer Nature or its licensor holds exclusive rights to this article under a publishing agreement with the author(s) or other rightsholder(s); author self-archiving of the accepted manuscript version of this article is solely governed by the terms of such publishing agreement and applicable law.